Application of the XBeach-Gravel Model for the Case of East Adriatic Sea-Wave Conditions

Bogovac, Tonko; Carević, Dalibor; Bujak, Damjan; Miličević, Hanna

Article

Application of the XBeach-Gravel Model for the Case of East Adriatic Sea-Wave Conditions

Tonko Bogovac *, Dalibor Carević, Damjan Bujak and Hanna Miličević

Faculty of Civil Engineering, University of Zagreb, 10000 Zagreb, Croatia
* Correspondence: tonko.bogovac@grad.unizg.hr; Tel.: +385-1-4864-452

Abstract: Croatia's coast located on the eastern Adriatic is rich with small gravel beaches with limited fetch. This leads to a specific low-energetic wave climate compared to most other beaches, while their gravel composition makes them unique. Most management of these beaches is performed without understanding the sediment transport occurring on the beaches. XBeach-Gravel is a numerical model capable of simulating bed-level change on gravel beaches, but lacks validation in the case of low significant wave height (under 2.5 m) and low peak periods (under 6 s), conditions that are present on the eastern Adriatic. Based on measurements performed in both laboratory conditions in a water canal in Hannover and actual storm wave conditions on Ploče beach, calibration of the model is performed. Model results are compared between laboratory conditions and field conditions for comparable wave conditions. XBeach-Gravel can simulate low-energetic events resulting in berm formation and berm buildup with a high Brier skill score if calibrated. Simulation of laboratory conditions requires high transport coefficient values and shows more sediment transport than similar wave conditions in the field. Calibration for field conditions is dependent on geodetic survey data capable of isolating wave events with dominant cross-shore transport, but once calibrated, XBeach-Gravel can achieve good to excellent Brier skill score values in simulating sediment change in low-energetic wave conditions on the eastern Adriatic.

Keywords: XBeach; gravel; beach nourishment; Adriatic; erosion

1. Introduction

While the world's coast is often made of long sandy beaches, Croatia's Adriatic coast contains many small and fetch-limited gravel beaches. These beaches are the workforce of the country's tourism industry [1] and nevertheless not managed on a national strategic or legislative level [2]. This in combination with beach management being delegated to local municipalities presents a few problems. As in the rest of the world, the dominant management practice used to remedy erosion due to wave events is nourishment [3]. Nourishment in general is easily scalable and ecologically sound [4] but also mostly unregulated in Croatia. This leads to Croatia's beach nourishment being biennial and using little sand and/or gravel. In comparison, other European countries nourish sand beaches on decadal time scales and with 10–100 times more sediment [3] than Croatia. Using inadequate sediment for nourishment was shown to reduce beach longevity, so careful selection of sediment for nourishment should be standard practice [5]. Unfortunately, mismanaged nourishments with gravel containing mud and clay that pollute the local coast are still being performed in Croatia. Additionally, Croatia has no obligatory strategic beach monitoring or management planning and so none is performed, despite such techniques being relatively inexpensive and easily available today [6]. They could also provide feedback to municipalities about the impact and quality of the nourishments that are performed [7].

While the growing tourism needs put constant pressure on municipalities and their beaches to satisfy ever rising visitor standards, the impact of climate change also looms [8]. Croatia's coast and beaches are oriented to the southwest and are known for strong Bora

(NE) and Sirocco (SE) winds, in which Sirocco is usually blamed for the loss of sediment on the beach, despite the limited fetch. Beaches are under the influence of wave event intensity and frequency that cause erosion of the shore—both of which are set to change with rising greenhouse gas emissions. In a warming climate, the Adriatic wave events, with the dominant Bora and Sirocco winds, will become slightly less common and intense [9,10], resulting in lower significant wave heights reaching gravel beaches, even in the worst climate "business as usual" RCP8.5 scenario [11–13]. Additionally, storm surges on the Adriatic, most famous for causing flooding in Venice when combined with high wind waves, are not changing much in the future as well [14], despite rising emissions following a RCP8.5 scenario. While this is good news for climate adaptability of Croatia's shore and beaches, rising sea levels are still expected and will be catastrophic—even with a slight decrease in wind speeds and without change in storm surge intensity. With predictions for year 2100 having increased sea levels of 0.44 to 0.75 m (compared to the 1995–2014 period) [8,15,16] and with extreme sea level reaching up to 1.2 m and becoming a commonly occurring event instead of rare, once in a hundred years event [17,18], constant evaluation and improvement of beach management practices is needed.

With no systematic data on beaches, no national monitoring systems in place, and with no clear legislature or strategy on nourishment and beach management, the room for improvement is both great and debilitating. Even in such conditions, there are tools and data available to improve the quality of nourishment and management projects on the coast, such as artificial neural networks and the more traditional numerical models. Artificial neural networks show great promise in all fields, and have been used to predict material volumes needed for nourishment on the Croatian coast [19]. However, process-based numerical models are still used predominantly, but almost all such models are focused on sandy coasts. XBeach-Gravel is a numerical model developed specifically for the simulation of morphological response of gravel beaches to wave events [20]. XBeach-Gravel is a derivative of XBeach, a numerical model for simulation of impact of storm events on sandy coasts. XBeach was modified into XBeach-Gravel with the inclusions of nonhydrostatic pressure correction term and with a groundwater transport module [21], and later on with a sediment transport module [20]. All three modifications allowed XBeach-Gravel to predict sediment change due to storm waves for a range of validation cases, even without site specific calibration [20].

XBeach-Gravel has since been used for mainly very energetic storm events on coasts with significant wave heights reaching 10 m and peak periods of 10 s [22], but also for a development of a parametric model to estimate barrier volume change on storm impact [23] and for superior empirical equations for wave runup [24]. One-dimensionality is its limiting factor, not allowing for simulation of longshore processes, but the work of Bergillos et al. [25] show how it can be coupled with a parametric longshore transport formula to provide good results. Xbeach-Gravel is even being used to investigate the response of mixed-sand gravel beaches to storms [26]. However, not much modeling and validation of the model for the case of coarse-grained gravel beaches has been performed [27], especially for the case of the Adriatic where gravel beaches are common, waves are fetch-limited, and storms are less energetic.

Following these findings, a clear gap is presented for the impact of low significant wave height and low peak frequency waves on the gravel coast—conditions that are common on the eastern Adriatic. McCall et al. [20] concluded that XBeach-Gravel can represent fairly the impact of such waves in laboratory conditions for the case of the BARDEX experiment [28], and that a site specific calibration of hydraulic conductivity and transport coefficients could increase the model's accuracy. To test this, XBeach-Gravel is calibrated for the case of low significant wave heights in the laboratory conditions—the *Grosser Wellenkanal* in Hannover from the work of López de San Román-Blanco et al. [29]. These results are compared with field measurements of similar waves on Ploče beach near Rijeka, noting the differences in the model's capability to simulate field and laboratory

conditions, and using XBeach-Gravel that accounts for groundwater transport, unlike previous attempts at simulation of storms on Ploče beach [30].

Simulation of wave events on Ploče beach in this paper outlines a calibration procedure for use on other similar beaches, while the calibrated coefficients are used to evaluate the model's capability to represent berm formation and wave runup. This procedure can then be used to evaluate the effectiveness of beach nourishment or the resilience of existing and constructed beaches to climate change and increased sea levels.

2. Materials and Methods

Calibration of the XBeach-Gravel model was performed on two different data sets. The first data set represents the experiments performed on a large wave channel (GWK, short for *Grosser Wellenkanal*) at the Coastal Research Center in Hannover, Germany, by López de San Román-Blanco et al. [29], while the second data set represents two wave events on Ploče beach near Rijeka, Croatia. The following subsection provides further details on the two data sets, while the last subsection explains the Brier skill score used to evaluate model results.

2.1. GWK Data Set and Numerical Model Setup (Laboratory Conditions)

Data collected from the GWK experiment is described in the paper by López de San Román-Blanco et al. [29]. The tests from López de San Román-Blanco et al. [29] used for calibration in this article were performed on Beach I, a gravel-only beach with sediment size between 16 and 32 mm, and median sediment size of 21 mm, sourced from interglacial rivers, and set on top of a impermeable asphalt layer with a slope of 1:6. The beach was constructed in a flume 309 m long, 7 m deep, and 5 m wide, allowing for a 1:1 scale conditions. The beach height was 6.5 m while the entire beach spreads 80 m in length; the water level was set at 4.7 m. The water level used also presented a limit to significant wave heights—half the water-level depth—any higher than that and waves would interact with the bottom at the source. The gravel beach layer had a slope of 1:8 with at least 2 m of depth (before reaching asphalt).

The beach was not reshaped after each test, meaning the resulting profile from one experiment was the initial beach profile for the next successive experiment. Tests from López de San Román-Blanco et al. [29] used for calibration in this paper are Test 1, 2, and 3, as summarized in Table 1.

Table 1. Key parameters of the three tests performed by López de San Román-Blanco et al. [29] in the GWK at Hannover: significant wave height (Hs), peak period (Tp), duration of the tests, and wave steepness (ratio of wave height to wave length). Other parameters used for model setup can be found in Appendix A.

	Test 1	Test 2	Test 3
Hs (m)	0.6	1	1.2
Tp (s)	3.22	4.14	4.48
Duration (s)	8400	7200	7800
Steepness		0.05	

Detailed model setup used to simulate the three tests is explained in Appendix A. Hydraulic conductivity (k_x) and transport coefficient (γ) parameters were calibrated with the intention of finding the combination of values for which the model result achieved the highest Brier skill score (explained in Section 2.3). Best values of the two parameters were selected among 52 combinations of hydraulic conductivity values (k_x) 0.01, 0.02, 0.034, 0.048, 0.062, 0.076, 0.09, 0.1, 0.2, 0.3, 0.4, 0.5, and 0.6 m/s, and transport coefficient values (γ) 0.5, 1, 2, and 3.

2.2. Ploče Beach Data Set and Numerical Model Setup (Field Conditions)

Second calibration of XBeach-Gravel was performed on a data set collected from measurements on Ploče beach (45.341000° N, 14.370514° E), which is in the western part of Rijeka. Ploče was constructed in 2011 as a part of the swimming pool complex above the beach when 2 natural embayments were transformed by the construction of 3 groins, a sill, a promenade behind the beach, and by the addition of D_{50} 32 mm gravel. Ploče is also nourished with gravel sediment on a yearly basis by the City of Rijeka following the redistribution and loss of sediment from winter wave events, primarily the ones from sirocco, a strong and constant wind from the southeastern direction. Ploče is oriented toward the southwest or ~219° (all angles referenced originate from north with clockwise direction being positive), with the beach stretching perpendicularly and facing relatively high sirocco waves formed on an effective fetch of about 16 km for the direction 135° ± 45°. Calculation of beach orientation is explained in Appendix D. All calibration and simulations were performed on the westernmost profile of the beach, displayed in Figure 1 and labeled as Profile 1. Papers by Lončar et al. [30,31] showed that incoming waves are directed parallel to Profile 1 (facing 192°) due to refraction and the influence of the western groin, while the middle groin shields the profile from waves below 160°, thus making Profile 1 suitable for calibration described in this paper.
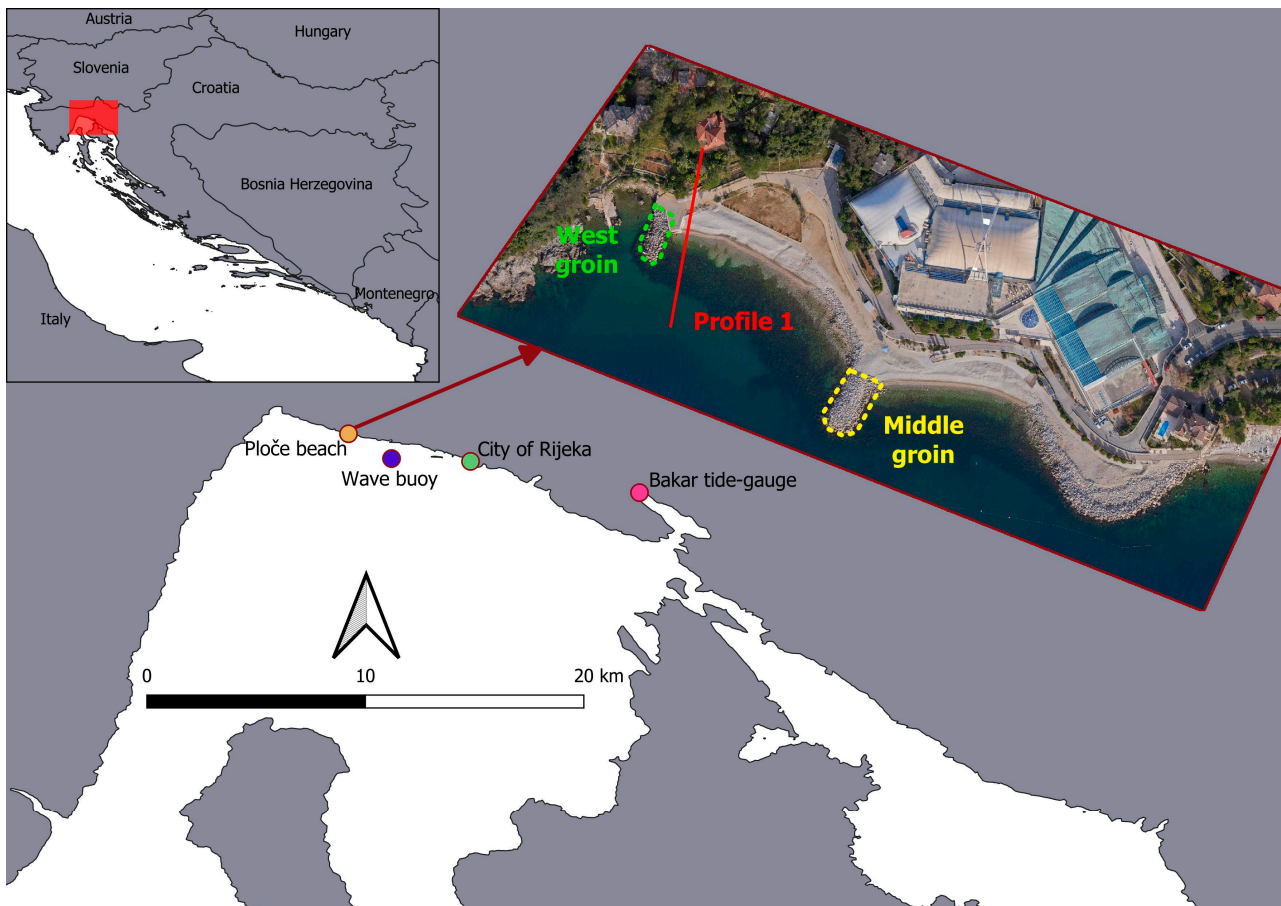

Figure 1. Map showing the relative location of Ploče beach to the wave buoy, Bakar tide-gauge, and the city of Rijeka, and displaying Ploče beach from the air with Profile 1 displayed with a red line.

Incoming waves were measured on a wave buoy (Datawell Waverider MkIII) located approximately 2.5 km southeast of Ploče; the buoy provided 30 min of wave statistics (significant wave height, peak period, wave direction and spreading) for the period from December 2019 until February 2021. During that time, 19 surveys of the beach were performed by the Faculty of Civil Engineering, University of Rijeka; details of the surveys

performed can be found in the paper by Tadić et al. [32], while tide-gauge data for the buoy measurement period was provided by the Department of Geophysics, Faculty of Science, University of Zagreb, for the station in Bakar, about 13 km southeast of Ploče beach.

The beach was also continuously monitored with an Argus-type video monitoring system consisting of a camera setup overlooking the beach and taking automated high-resolution images for analysis [33]. Such a system was set up starting from October 2020 allowing for wave-runup measurement on Ploče beach to measure wave runup and results are published in the paper by Bujak et al. [34]. The video monitoring system sampled images of the west beach cell (between the west and middle groins shown in Figure 1) with a frequency of 4 Hz and for 12 min intervals during wave events, but only in daylight. Following analysis, the images allowed for determination of the water elevation and wave runup.

Analyzing wave data, 17 separate wave events were identified between geodetic survey 11 and 18 from the 1 October 2020 and 14 January 2021 based on significant wave height (Hs). Identifying criteria for a wave event were set at Hs surpassing the 90th percentile (0.45 m), while the event beginning and end were set at the crossing of the 80th percentile (0.27 m). Wave events identified by these two criteria were further labeled following the naming scheme: *Gxx_Gyy_Kzz*, where *Gxx* and *Gyy* denote the two geodetic surveys in between which the wave event took place, while the *Kzz* denotes the wave event in between the two surveys. All wave events are listed in detail in Appendix B.

Comparing sediment changes on the beach profile for surveys 11–18 reduced the number of suitable wave events for calibration to only the ones between surveys 12 and 15; those surveys show less than 1 m of net sediment change on the profile, which implies predominant cross-shore transport or redistribution of sediment along the profile. Net sediment change was estimated by subtracting the later profile from the earlier one, and then summing the results for all coordinates. Ideally, profile net sediment change should be close to zero as that would imply only cross-shore sediment redistribution. Large net sediment change on the profile implies significant longshore sediment transport, which is unsuitable for calibration as it cannot be accounted for by the one dimensional, cross-shore model. Net sediment changes for all surveys are reported in Appendix C.

The criteria above reduced the number of wave events to 6, out of which no wave runup was measured for the two events between survey 14 and 15—resulting in only 4 remaining wave events suitable for calibration between surveys 12, 13, and 14. All remaining 4 events had waves arriving at the beach from the direction of 160° and above for most of the wave event, avoiding the middle groin. Additionally, refraction caused incoming sirocco (SE) waves to arrive perpendicularly to the shore [30,31].

Between geodetic surveys 12 and 13, only one wave event occurred—wave event G12_G13_K1 with Hs of 0.7 m, Figure 2, left panel. Event G12_G13_K1 started on 6 October 2020 at 15:00 and ended 18.5 h later on 7 October at 9:30. Runup was measured on the evening of the 6 October and the morning of the 7 October, as most of the event occurred during the night, not allowing the video monitoring system to measure wave runup. Average significant wave height for the wave event was 0.47 m with a maximum of 0.7 m, with the average peak period of 3.1 s. This wave event is comparable to Test 1 with a significant wave height of 0.6 in the GWK.

The second two surveys, 13 and 14, had 3 separate wave events with increasing significant wave height: 0.53, 0.78, and 1.28 m. The wave event with the highest Hs had the dominant effect on profile change [35], so only the G13_G14_K3 event was used for calibration, while the two preceding events were not. Average significant wave height of G13_G14_K3 was at 0.89 m with a maximum of 1.28, comparable to Test 3 in the GWK, and the average peak period was 3.9 s. The tide slowly increased from around 0.3 m up to 0.6 m at the end of the event.
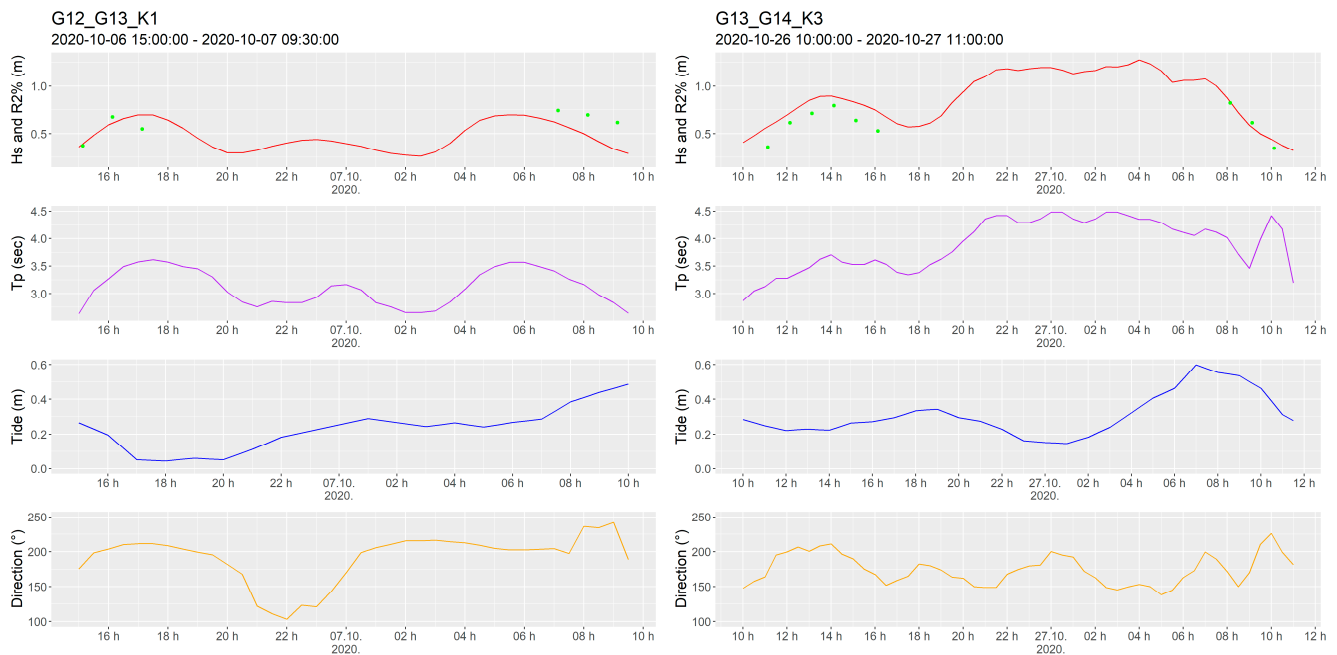
Figure 2. Parameters of wave events G12_G13_K1 (**left**) and G13_G14_K3 (**right**) used to simulate the wave events using XBeach-Gravel. From top to bottom: significant wave height (Hs) determined by the wave buoy (red line) and 2% exceedance rate of wave runup measured by the video monitoring system (R2%, green dots); peak period or Tp measured by the wave buoy (purple line); mean sea level change due to tides as measured on the Bakar tide-gauge (blue line), and wave direction (yellow line) also measured on the wave buoy.

The events G12_G13_K1 and G13_G14_K3 were used to calibrate the model by assessing the model's capability to predict profile changes (recorded on the profile shown by a red line in Figure 1). Data for both wave events were smoothed using a 1.5 h rolling mean to smooth changes in wave period measurements. An ensemble of models with combinations of hydraulic conductivity (kx) values 0.05, 0.1, 0.2, 0.3, 0.4, and 0.5, and transport coefficient (γ) values 0.25, 0.5, 1, and 1.5 were run to represent a wide spectrum of possible values. Detailed model setup can be found in Appendix B, while all simulations on Ploče beach used a non-erodible layer for the depths below 1.5 m (or for x coordinates below 55). The part of the beach profile below 1.5 m is built of rock material with larger mean diameter and is not erodible, as found by the geodetic surveys on Ploče presented in [32]. Brier skill scores were calculated for each simulation and combination of hydraulic conductivity and transport coefficient; the combination with the highest average Brier skill score (of the two tests) was considered as appropriate for Ploče beach.

With the parameters of hydraulic conductivity and transport coefficient determined by calibration on events G12_G13_K1 and G13_G14_K3, further analysis was performed. The two events used for calibration (G12_G13_K1 and G13_G14_K3) were compared to the similar two events in the GWK (Test 1 and Test 3) based on their comparative significant wave height.

Additionally, simulation of wave event G17_G18_K3 was performed to validate the model for the case of wave overtopping, seen in Figure 3, and to compare changes in the beach profile caused by a similar wave event analyzed by Lončar et al. [30]. The event G17_G18_K3 with a maximum significant wave height of 2.3 m was preceded by and followed by an additional 2 events with a maximum significant wave height of 1.05 m and less, rendering it unsuitable for model calibration.
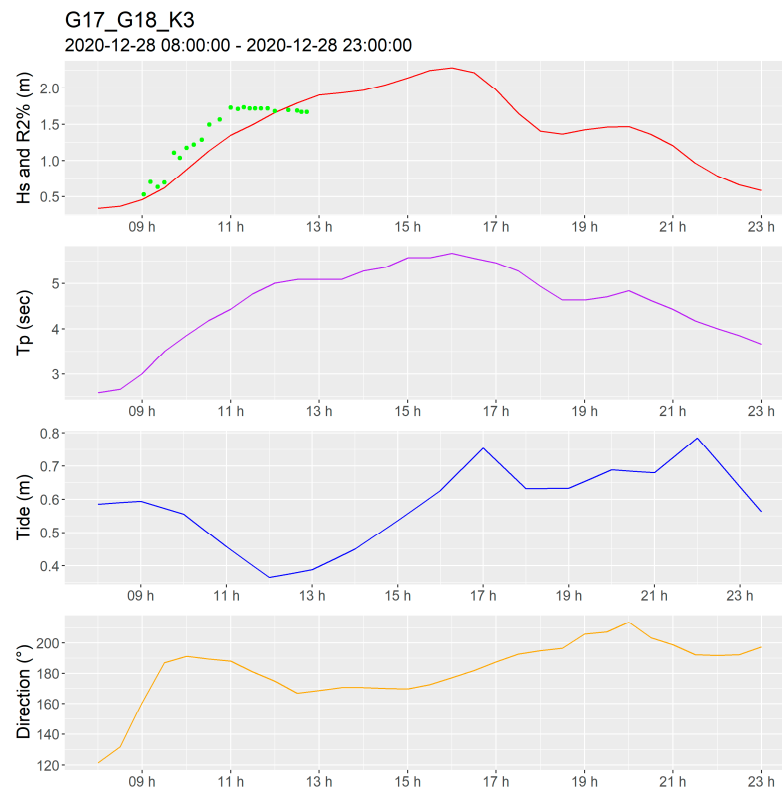
Figure 3. Parameters of wave event G17_G18_K3 used to simulate the event using XBeach-Gravel: significant wave height (Hs, red line) and 2% exceedance rate of wave runup (R2%, green dots); peak period (Tp, purple line); mean sea level change (blue line), and wave direction (yellow line).

Wave runup shown in Figures 2 and 3 is represented by green dots and is comparable to significant wave height, which is to be expected. Poate et al. [24] noted the ratio of wave runup to significant wave height depends on location and can be in the range 2 to 0.4. Poaet et al. [24] also note the ratio can change during the same wave event as wave conditions, beach profile, and energy dissipation change.

2.3. Brier Skill Score

In order to determine the quality of model prediction compared to measured results and against a baseline prediction, Brier skill score is commonly used in coastal modeling [20,26,36]. As the Brier skill score value approaches 1, so does the model prediction approach the actual desired (measured) result. In contrast, a Brier skill score of 0 implies that the model is equally good in predicting the desired result as is our referenced baseline prediction, while a negative value means the model is worse than the baseline. The baseline used in this paper is the initial geodetic survey (before the event) against which the model prediction is compared. The model prediction should approach the measured geodetic survey (after the event). According to Table 2, BSS values above 0.6 imply good model prediction [37].

Table 2. Qualification of different Brier skill score ranges according to van Rijn et al. [37].

Brier Skill Score	Qualification
0.8–1	Excellent
0.6–0.8	Good
0.3–0.6	Fair
0–0.3	Poor
<0	Bad

Brier skill score is calculated using the absolute change prediction error at all points along the profile and symbolized as $|\epsilon_{\Delta\zeta}|$. This is determined as the maximum of the absolute difference between the bed-level change in the model (for each point) and the bed-level change in the measurements (also for each point) from which the instrument error (ϵ_0) is also deducted. If this is less than zero, then the value of this error $(|\epsilon_{\Delta\zeta}|)$ is set to zero.

$$|\epsilon_{\Delta\zeta}| = \max(|\Delta\zeta_{modeled} - \Delta\zeta_{measured}| - \epsilon_0, 0) \tag{1}$$

Having determined this error, Brier skill score can be calculated as follows:

$$BSS = 1 - \frac{\frac{1}{n}\sum_{i=1}^{n}|\epsilon_{\Delta\zeta}|_i^2}{\frac{1}{N}\sum_{i=1}^{n}(\Delta\zeta_{i,measured})_i^2} \tag{2}$$

3. Results

3.1. XBeach-Gravel Calibration for the GWK Data Set (Laboratory Conditions)

The three tests from Table 1 performed at the GWK and then simulated using XBeach-Gravel used 52 different combinations of the transport coefficient (0.5, 1, 2, and 3) and hydraulic conductivity (0.01, 0.02, 0.034, 0.048, 0.062, 0.076, 0.09, 0.1, 0.2, 0.3, 0.4, 0.5, and 0.6 m/s) to determine the highest obtainable BSS. Resulting BSS values in relationship to hydraulic conductivity and transport coefficient are displayed in Figure 4 for the GWK.
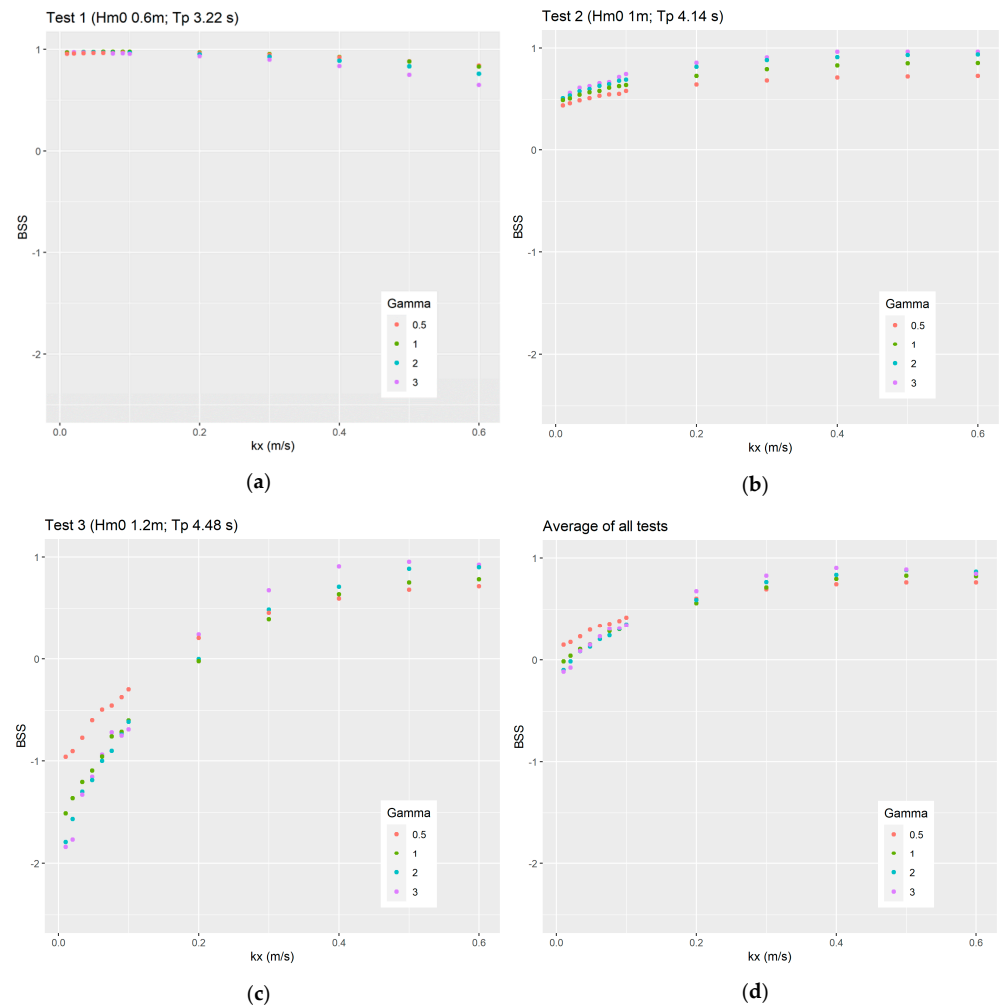

Figure 4. Relationship between hydraulic conductivity (kx), Brier skill score, and transport coefficient (gamma) for (**a**) Test 1, (**b**) Test 2, and (**c**) Test 3, and for (**d**) the averaged Brier skill score for all three tests.

Hydraulic conductivity could be estimated from grain size [24,38]; however, hydraulic conductivity was determined by calibration similar to the one performed by Brown et al. [26] rather than from grain size. The remaining transport coefficient is a free parameter that requires calibration.

For Test 1, any of the hydraulic conductivity and transport coefficient values used for calibration result in high values of BSS, with a very gradual decline in BSS values with an increase in hydraulic conductivity and transport coefficient values—but never resulting in BSS lower than 0.64 for parameters used here. Test 2 shows the opposite behavior, BSS values increase slightly more steeply than in Test 1 with the increase in hydraulic conductivity and transport coefficient values. Additionally, BSS values are generally lower for this test, with the average BSS value for the entire calibration being lower for about 0.3 in comparison with Test 1 average BSS, primarily because of the reduction in BSS values for lower hydraulic conductivity.

In Test 3, the gradient caused by both hydraulic conductivity and transport coefficient is quite larger. Most simulations with hydraulic conductivity below 0.2 m/s have negative BSS values, implying that the modeled profile is worse than using the initial profile as a prediction. Above a kx of 0.3 m/s, BSS values are in the range of good or excellent.

Since all three tests used the same set of calibration parameters and because XBeach-Gravel is intended to be used with little to no site-specific and no event-specific calibration, BSS values could be averaged for all three tests for each of the 52 unique combinations of hydraulic conductivity and transport coefficient values in order to determine the combination of kx and γ with the highest BSS. The resulting averaged BSS values are also displayed in Figure 4d. Averaged BSS is highest for hydraulic conductivity of 0.4 m/s and transport coefficient of 3 and is valued at 0.9; all three tests with these parameters are displayed in Figure 5.
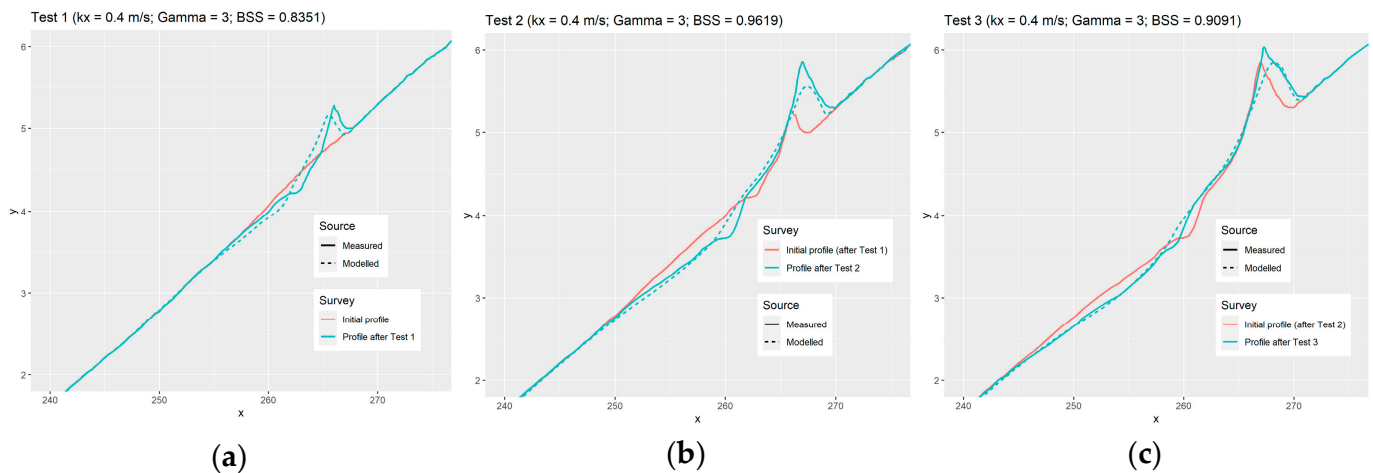

(a)   (b)   (c)

Figure 5. Modeled and measured profiles for three tests with the model using parameters resulting with the highest BSS on average for all three tests, hydraulic conductivity set at 0.4 and transport coefficient set at 3: (**a**) Test 1, (**b**) Test 2, and (**c**) Test 3, where the red line presents the initial profile for the test, full blue line represents the measured profile after the test, and the blue line with breaks represents the modeled profile after the test.

Test 1 uses a low significant wave height of 0.6 m, which causes berm height formation of 0.45 m, as visible in Figure 5a, while XBeach-Gravel does form a similar berm in size (0.38 m), its position is transported slightly toward the offshore, resulting in a lower BSS value. Upon a visual inspection of the resulting profiles, it can be concluded that the model does provide good qualitative results.

In Test 2 (Figure 5b), the model predicts a 0.56 m berm, which is lower than the 0.88 m berm formed by the 1 m significant wave height, but the location of the berm is predicted accurately. Similarly, for Test 3 in Figure 5c, the location of the new 1 m berm is

predicted correctly, while the model berm of 0.75 m is still underpredicted. According to McCall et al. (2015), the model is capable of predicting the influence of low-energy waves causing berm formation in a qualitative sense, but the quantitative skill of the model is not high, with a median BSS of 0.54 for the two cases studied.

However, the results for the three tests shown in Figure 5 show the model is, with site specific calibration, capable of achieving an average BSS of 0.9 for the case of berm formation in low-energetic wave conditions. It should be noted that McCall et al. [20] used a transport coefficient of 1, while this analysis uses an even higher value, 3, to achieve high BSS results for laboratory conditions. High transport coefficient values for laboratory conditions could be caused by the use of fluvial sediment confined to a narrow water canal, allowing sediment to be more mobile than in field conditions. The model is also less sensitive to the selection of hydraulic conductivity values between 0.2 and higher, perhaps because above 0.2 m/s the infiltration rate of water is sufficient enough that higher values make no large difference in the simulations.

3.2. XBeach-Gravel Calibration for the Ploče Data Set (Field Conditions)

The same procedure used for the GWK was repeated for the calibration of the Ploče data set for two wave events, G12_G13_K1 and G13_G14_K3. Twenty-four simulations were performed for both events using a combination of hydraulic conductivity values (0.05, 0.1, 0.2, 0.3, 0.4, and 0.5) and transport coefficient values (0.25, 0.5, 1, and 1.5). For every simulation, a BSS was calculated to evaluate the effectiveness of the parameter combination. BSS compared the after event profiles from the simulation to the profile measurements on the beach.

Figure 6 compares BSS values for different parameter combinations for both events. BSS values increased with an increase in hydraulic conductivity values and with a decrease in the transport coefficient. The dominant impact on BSS was from the transport coefficient whose decrease resulted in less mobile sediment. As the analysis of profile change in later figures will show, sediment in the field conditions of Ploče beach is not as mobile as in laboratory conditions, so a lower value of transport coefficient is needed.
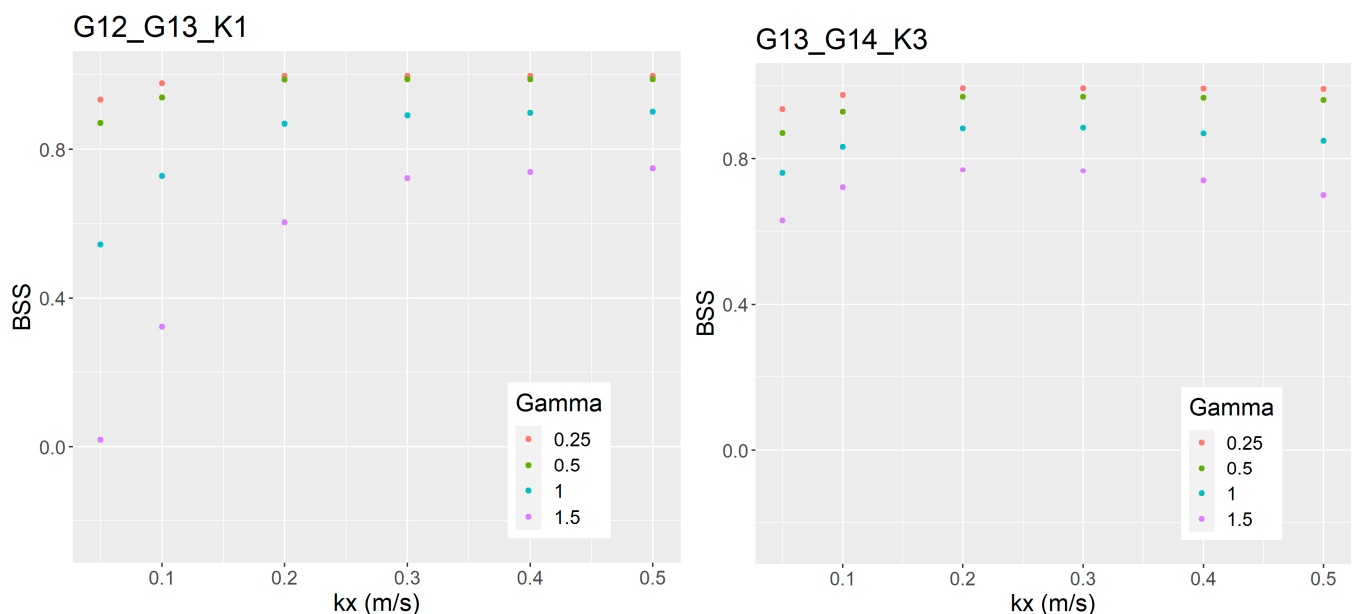

Figure 6. Brier skill score values for simulations of events G12_G13_K1 (**left**) and G13_G14_K3 (**right**) for different hydraulic conductivity and transport coefficient values.

Peak BSS values for the beach Ploče data set were achieved for hydraulic conductivity above 0.2 m/s and transport coefficient of 0.5 and less, resulting in a large parameter space capable of simulating profile changes caused by wave events.

Average BSS values for both tests and each parameter combination, displayed on Figure 7 show the highest BSS value for the combination of hydraulic conductivity of 0.3 m/s and transport coefficient of 0.25. Wave event simulations with those parameters are further analyzed next.
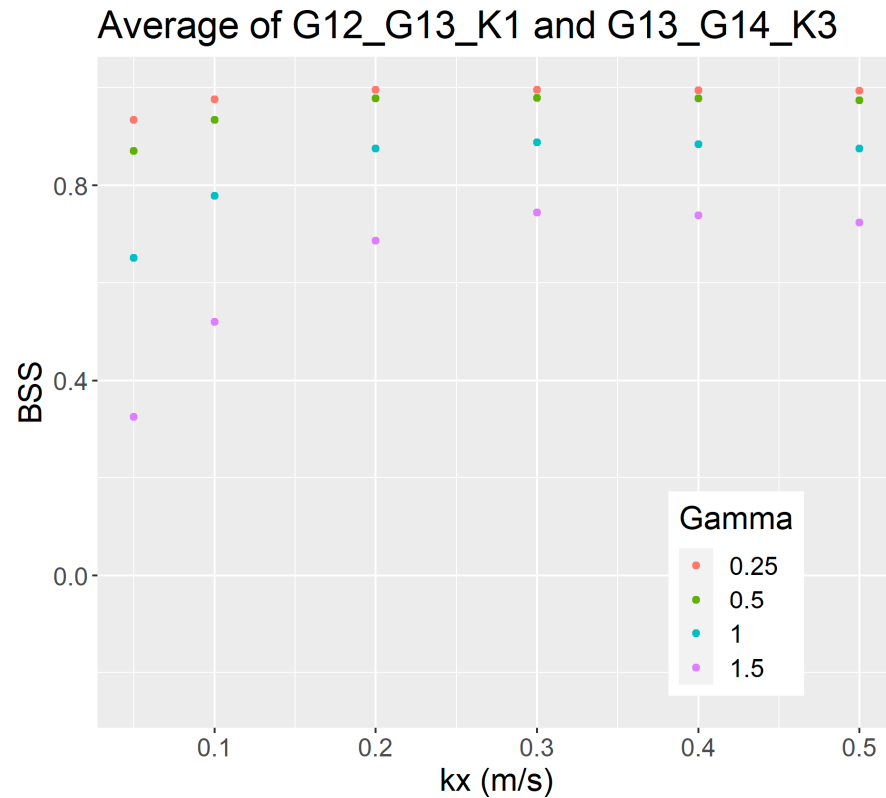

Figure 7. Average of Brier skill scores for wave events G12_G13_K1 and G13_G14_K3 for each combination of different hydraulic conductivity and transport coefficient values. Highest Brier skill score value (of 0.995) is obtained for the combination of hydraulic conductivity 0.3 m/s and transport coefficient 0.25.

Wave event G12_G13_K1 causes only small changes in the sediment profile on Figure 8: two berms (red color, before x = 60 and x = 65) have succesfully redistributed along the profile by waves with significant wave height of 0.6 meters. Resulting high BSS value implies the model predicted the measured sediment change on the profile correctly, despite the changes on the profile being small. This is in stark contrast to the results of Test 1 where a comparable significant wave height produces a berm 0.45 m high in laboratory conditions, underlying again the difference of field and laboratory behaviour of gravel beaches. It should be noted that Hs of 0.6 meters lasted for 2.5 hours in Test 1, while G12_G13_K1 had average Hs of about 0.6 meters for 6 hours in total and still did not produce sediment change comparable to Test 1.

The right panel in Figure 8 shows 2% exceedence rate of wave runup (R2%, both measured and modeled) along with significant wave height (Hs). Modeled R2% and measured Hs show good correlation, while the measured R2% exceeded significant wave height and modeled R2% in the second part of the event.

The second wave event, G13_G14_K3, includes a higher significant wave height of 1.25 m at its highest, comparable to Test 3 in the GWK. This event caused more change in the profile, as seen in Figure 9, moving the previously existing berm higher. The model successfully replicates this change while eroding a small part of the sediment further down—a feature that was not seen in the profile measurements. Significant wave height and the measured and modeled 2% exceedance rate of wave runup show good correlation.
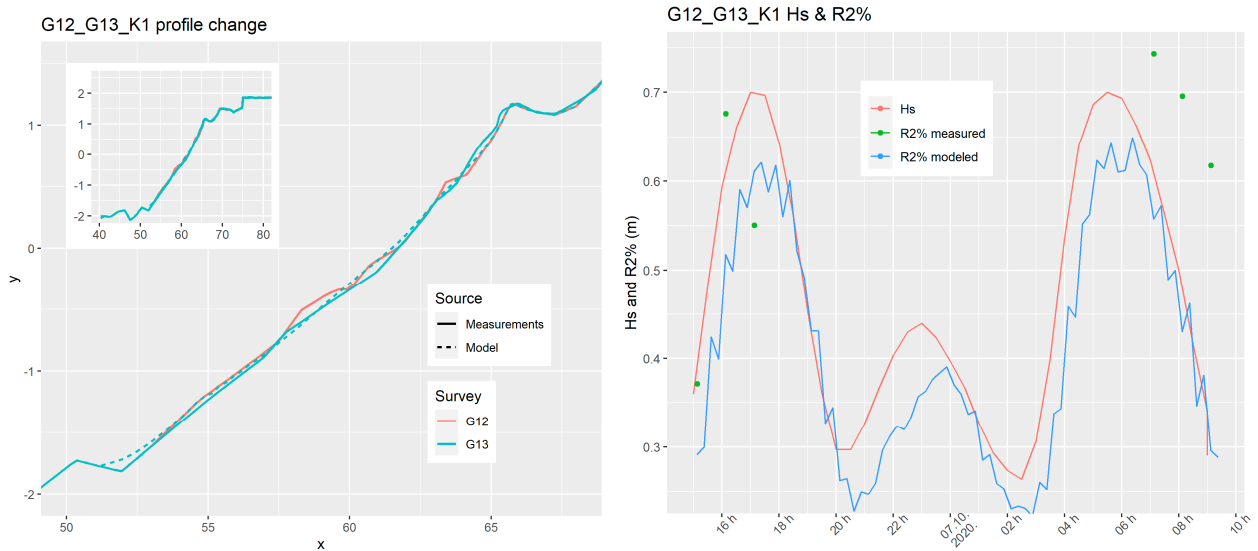
Figure 8. Simulation of G12_G13_K1 wave event results: changes in sediment profile (**left**) and wave runup during the event (**right**). No major sediment change occurred on the profile; simulated wave runup (blue line) follows the significant wave height (red line) while measured runup (blue dots) is slightly underpredicted.
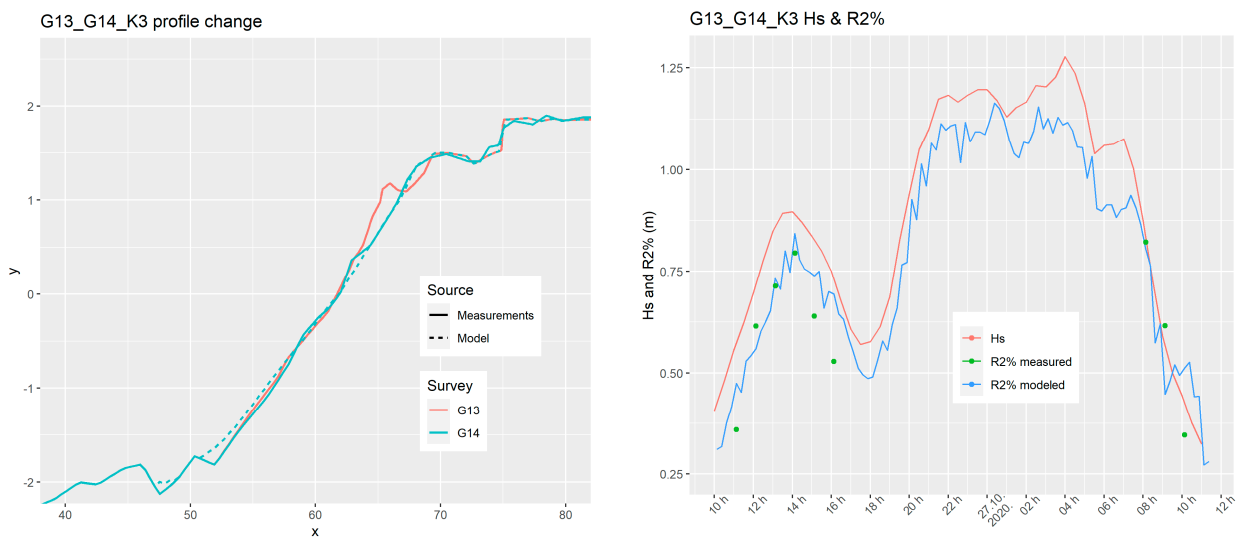

Figure 9. Simulation of G13_G14_K3 wave event results: changes in sediment profile (**left**) and wave runup during the event (**right**). Profile change shows crest buildup, which the model correctly predicts (dashed and solid cyan). Modeled (blue line) and measured (green dot) wave runup are in agreement and are less than the measured significant wave height (red line).

3.3. Validation for the Case of Wave Overtopping

Additionally, an event with a significant wave height of 2.28 m, G17_G18_K3, was also simulated in order to compare the event with a similar wave event described by [30,31]. The model is capable of reproducing wave overtopping, as seen in Figure 10, right panel.

Measured wave runup on Figure 10 is increasing with the increase in significant wave height until it reaches 1.75 m at about 11:00 which, in combination with the tide increasing the sea surface level for an additional 0.4 m, results in waves higher than the berm on the profile.
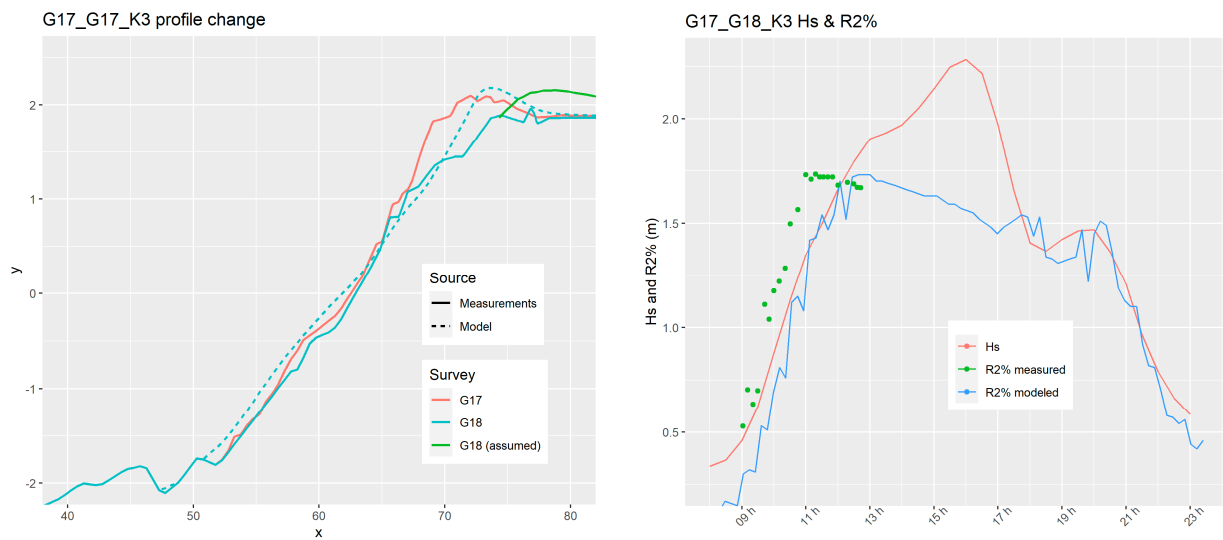
Figure 10. Simulation of G17_G18_K3 wave event results: changes in sediment profile (**left**) and wave runup during the event (**right**). The model predicts the profile change in the form of large crest buildup (dashed cyan), while it is assumed that the wave event resulted in the crest being further right (solid green), and that in both cases, excess material onshore was cleared by the City of Rijeka. Right figure shows modeled wave runup (blue line) and measured wave runup (green dots) are in agreement and less than the measured significant wave height (red line) due to overtopping.

Profile changes caused by the G17_G18_K3 event suggest the event resulted with a large crest buildup, while some of the material is eroded and spread out evenly below the waterline. This partially aligns with the conclusion of [30,31]; XBeach-Gravel clearly simulates expected sediment accumulation onshore; however it does also simulate some erosion of the material in the offshore direction not represented in [30,31]—subsequent lower-energy wave events after G17_G18_K3 could have moved the eroded material back onshore. The builtup crest and berm from the 17th survey and after wave event G17_G18_K3 are not visible on the 18th survey—the reason being that the crest material buildup on top of the beach after the G17_G18_K3 wave event was cleared by the communal department of City of Rijeka. This occurred on the morning of 9 January 2021, 5 days before the 18th geodetic survey took place, as seen at the bottom of Figure 11.

However, given previous results from [30,31] and based on Ploče beach being a pocket beach, the modeled movement of sediment onshore is probably underrated and should align closer to the assumed G18 profile (marked solid green in Figure 10). This could be achieved by accounting for an additional sea level increase of about 80 cm modeled as tidal increase, which is not presented in this paper. The tidal increase would account for pocket beaches (small beach, isolated and enclosed by headland that prevents longshore sediment transport) having increased wave setup in comparison to linear beaches (beaches not enclosed by headland where sediment usually transports in the longshore direction) and which XBeach-Gravel does not account for in the case of higher significant wave heights. Having geodetic surveys performed densely enough to isolate the impact of particular wave events would provide better understanding of XBeach-Gravel's capabilities to simulate pocket gravel beaches.

XBeach-Gravel shows quantitative agreement with other models when simulating sediment changes on Ploče beach, but its one-dimensionality presents a limiting factor as wave events need to be selected based on their reduced longshore transport. Additionally, the number of wave events between two subsequent geodetic surveys also limited our ability to account for the entirety of sediment changes. Still, XBeach-Gravel represents the only model intended to simulate gravel beaches and the aforementioned results demonstrate that it can be used for Croatia's wave climate and pocket beaches.
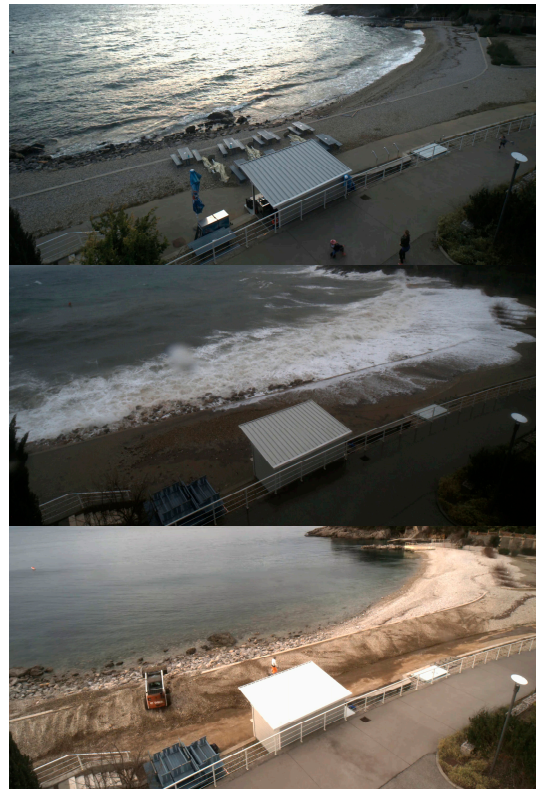
Figure 11. Images from the video-monitoring system depicting wave conditions during the G13_G14_K1 event (**top**), G17_G18_K3 event (**middle**) with visible overtopping on Profile 1, and workers removing the overwashed sediment on 9 January 2021 (**bottom**)—5 days before the 18th geodetic survey took place, and 2 weeks after wave event G17_G18_K3.

4. Discussion

XBeach-Gravel is a numerical model used for simulating storm impacts on gravel and mixed sand–gravel shores. While attempts have been made to simulate sediment transport on Croatia's gravel beaches with various models, XBeach-Gravel has not been used previously in this specific wave climate. Wave conditions typical for Croatian beaches include low-energy wave events resulting in berm formation or berm erosion, while crest buildup occurs in more energetic cases. This paper's purpose was to test XBeach-Gravel's ability to simulate such events in both field and laboratory conditions to demonstrate its applicability to Croatia's gravel beaches.

Previously, McCall et al. [20] showed that high-energy wave events can be simulated without site-specific calibration with a high BSS value of 0.75, which is considered good; however, the model's performance for low-energy wave events proved fair with a BSS of only 0.54. The authors of [20] also noted that BSS values for low-energetic events can be increased if site-specific calibration of the model is performed. Site-specific calibration of the XBeach-Gravel model for the case of the laboratory (GWK, Figure 4d) and field conditions (Ploče beach, Figure 7) performed and reported in this paper resulted in an excellent BSS of 0.9 for low-energetic events. The increase in BSS values for XBeach-Gravel achieved by site-specific calibration demonstrates that XBeach-Gravel can be used for the simulation of beach profile change due to storm events on the eastern Adriatic coast.

Calibrated parameters for laboratory conditions at the GWK are hydraulic conductivity (kx) of 0.4 m/s and transport coefficient (γ) of 3, while for field conditions on Ploče beach, they are 0.3 m/s and 0.25, respectively. Laboratory simulations performed at the GWK on 1:1 scale were replicated with Xbeach-Gravel with a high value of the transport coefficient γ. The calibrated parameters can be used to further model profile changes on Ploče gravel beach and to validate the obtained results on different beaches on the Adriatic.

Simulated laboratory and field wave conditions were comparable and showed that waves of about 0.6–0.7 m significant wave height have almost no impact on Ploče beach, while the same wave in the laboratory causes formation of a berm 0.45 m high for comparable grain size (GWK with 21 mm and Ploče with 20 mm). Both simulations of about 1.2 m significant wave height show crest buildup, but with more change occurring again in the laboratory conditions. The impact of waves with 0.6 and 1.2 m significant wave height on beach profile change is larger in the laboratory than in the field. The difference can be accounted for by the model with a substantial increase in the transport coefficient used.

In both wave events used for model calibration for field conditions on Ploče beach, the modeled wave runup agreed with the measured wave runup. Additionally, a wave event with a significant wave height of 2.3 m was also simulated once the model was calibrated. The model replicated the measured wave runup for this case, with wave overtopping being present.

This paper's limitations are primarily in the form of data available for research in field conditions. Field measurements on the Adriatic coast are rare and the geodetic measurements on Ploče beach should have been performed more densely in order to isolate particular wave events for analysis. This caused a reduction in the number of wave events available for calibration or analysis, reducing the study to only two wave events for calibration, and to only one storm event for analysis. A different design of planned measurements, such as performing measurement with more extreme weather-tolerant gear and right before and after wave events, would have allowed for more robust research. Another limiting factor was the present longshore transport on the Ploče beach, which reduced the choice of profiles for simulation. Longshore transport could be taken into account following the results of Bergillos et al. [25] by coupling a longshore sediment transport formulation to the model. Additionally, in the performed measurements on Ploče beach, there were no wave events with Hs above 2.3 m, still leaving a smaller research gap for modeling the impact of wave conditions on the Adriatic on gravel beach profile changes.

The results presented underline XBeach-Gravel's ability to model mild wave conditions (under 2.5 m Hs and less than 6 s Tp) both in the laboratory and in the field. Such wave conditions are common on the eastern Adriatic coast due to fetch-limited conditions, and so far have not been represented in research with Xbeach-Gravel, in which most tested wave events have been for Hs above 5 m and included Tp of 10 s or more [20,24,26,27]. While different numerical models have been used prior to simulate changes on Croatia's gravel coast, even on Ploče beach specifically [30,31], XBeach-Gravel is intended to simulate gravel beaches and incorporates groundwater transport processes, which is lacking in other models. Additionally, XBeach-Gravel is relatively simple to use and faster than full 3D models. These model characteristics, along with the model's capability to simulate wave events on the Adriatic demonstrated in this paper, present the model as a potential tool for informing beach management decisions prior to nourishment projects common in Croatia, where no planning or monitoring is usually performed. For example, XBeach-Gravel could be used to evaluate different beach profile constructions on artificial gravel beaches or to determine the rate of sediment loss in the future climate.

Appendix A

Table A1. All parameters used for simulation of Test 1, Test 2, Test 3, G12_G13_K1, G13_G14_K3, and G17_G18_K3.

Parameter Name	GWK—Test 1, 2 and 3			Beach Ploče—G12_G13_K1 and G13_G14_K3	Beach Ploče—G17_G18_K3
Profile parameter setup					
Minimum grid size (m)	0.1			0.1	0.1
Maximum grid size (m)	1			0.5	0.5
Minimum points per wavelength	40			60	60
Maximum offshore bottom level (m)	0			−2 (m) for both simulations	−4 (m)
Coordinates	Constructed profile of Beach I in the GWK and subsequent profiles after Test 1, 2, and 3			Geodetic survey 12 and 13, respectively	Geodetic survey 17
Wave parameters setup					
Spectrum type	Unimodal for all waves			Unimodal for all waves	Unimodal for all waves
Gamma	3.3 for all waves			3.3 for all waves	3.3 for all waves
Significant wave height (m)	Test 1	Test 2	Test 3	30 min average of Hs provided by the buoy measurements for each storm, smoothed by 1.5 h rolling average	30 min average of Hs provided by the buoy measurements for each storm, smoothed by 1.5 h rolling average
	0.6	1	1.2		
Peak period (s)	Test 1	Test 2	Test 3	30 min average of Tp provided by the buoy measurements for each storm, smoothed by 1.5 h rolling average	30 min average of Tp provided by the buoy measurements for each storm, smoothed by 1.5 h rolling average
	3.22	4.14	4.48		
Spreading	10 for all waves			30 min average of S provided by the buoy measurements for each storm, smoothed by 1.5 h rolling average	30 min average of S provided by the buoy measurements for each storm, smoothed by 1.5 h rolling average
Tide parameters setup					
Back boundary water level	Variable			Variable	Variable
Offshore water level (m)	Set to 4.7 m for the entire simulation			30 min interpolated data from the 1 h tide-gauge measurements at Bakar for each storm	30 min interpolated data from the 1 h tide-gauge measurements at Bakar for each storm
Parameters setup					
Duration (s)	Test 1	Test 2	Test 3	68,400/91,800	55,800
	8400	7200	7800		
Initial groundwater level (m)	0			0	0
Bottom aquifer (m)	0			0	0
D50—Median grain size (m)	0.021			0.02	0.02
Hydraulic conductivity (m/s)	0.01, 0.02, 0.034, 0.048, 0.062, 0.076, 0.09, 0.1, 0.2, 0.3, 0.4, 0.5			0.05, 0.1, 0.2, 0.3, 0.4, 0.5	0.3
Angle of repose (°)	35			35	35
Sediment transport formula	Van Rijn			Van Rijn	Van Rijn
Inertia coefficient (Ci)	1			1	1
Transport coefficient (γ)	0.5, 1, 2, 3			0.25, 0.5, 1, 1.5	0.25

Appendix B

Figure A1 displays 17 wave events from October 2020 until 14 January 2021 along with its defining significant wave height. Each event is noted on the figure. Additional details for each wave events are listed in Table A2.
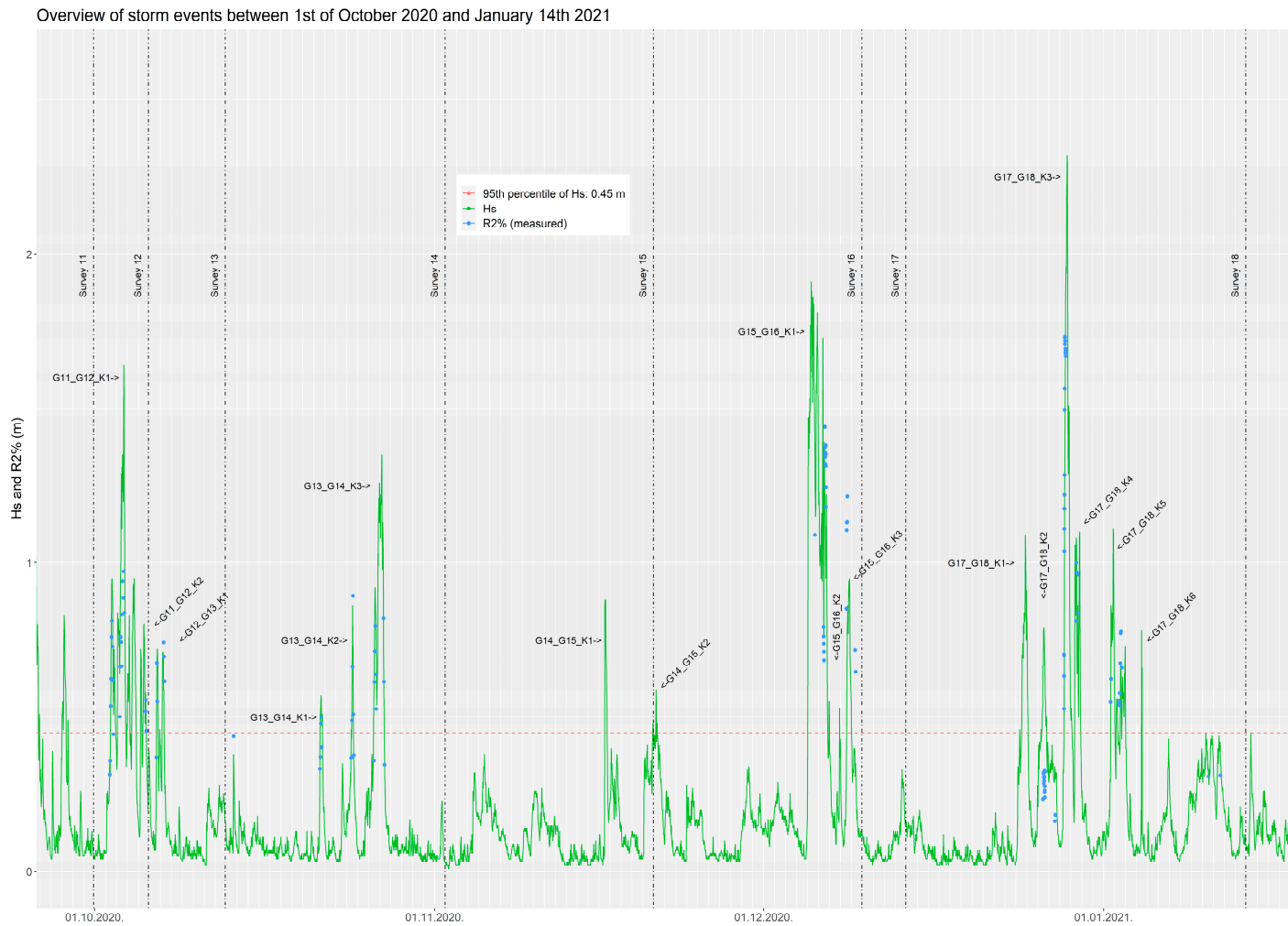
Figure A1. Significant wave height (Hs, green line) and 2% exceedance rate of wave-runup (R2%, blue dots) data displayed with vertical dot–dashed lines displaying the occurrence of geodetic surveys of the beach. Upon exceedance of the 90th percentile of significant wave height (0.45 m; red), a wave event was declared from the moment Hs increased above the 80th percentile (0.27 m) and declared finished once Hs decreased below the 80th percentile. Each wave event is annotated on the figure by its name.

Table A2. Additional details for each of the 17 wave events occurring from October 2020 until 14 January 2021.

Geodetic Surveys		Number of Wave Events	Net Sediment Change (m)	Start of Event	End of Event	Hs Max (m)	Average Wave Direction (°)	Runup Measurement
G11 1.10.2020.	G12 6.10.2020.	K1	2.64	2.10.2020. 08:00:00	4.10.2020. 20:00:00	1.64	187	Yes
		K2		5.10.2020. 04:00:00	5.10.2020. 20:00:00	0.8	195	Yes
G12 6.10.2020.	G13 13.10.2020.	K1	−0.02	6.10.2020. 15:00:00	7.10.2020. 09:30:00	0.72	191	Yes
G13 13.10.2020.	G14 2.11.2020.	K1	−0.57	21.10.2020. 12:30:00	21.10.2020. 20:30:00	0.57	184	Yes
		K2		24.10.2020. 08:00:00	24.10.2020. 16:00:00	0.86	199	Yes
		K3		26.10.2020. 10:00:00	27.10.2020. 11:00:00	1.35	182	Yes
G14 2.11.2020.	G15 21.11.2020.	K1	0.08	16.11.2020. 12:00:00	16.11.2020. 18:30:00	0.88	186	/
		K2		20.11.2020. 20:00:00	21.11.2020. 16:30:00	0.59	136	/
G15 21.11.2020.	G16 10.12.2020.	K1	11.11	5.12.2020. 00:00:00	7.12.2020. 04:00:00	1.91	177	Yes
		K2		7.12.2020. 21:30:00	8.12.2020. 01:00:00	0.53	200	/
		K3		8.12.2020. 12:30:00	9.12.2020. 10:30:00	0.95	182	Yes
G16 10.12.2020.	G17 14.12.2020.	/	−1.06			/		
G17 14.12.2020.	G18 14.1.2021.	K1	−5.15	24.12.2020. 03:00:00	25.12.2020. 05:00:00	1.09	199	/
		K2		26.12.2020. 04:00:00	27.12.2020. 17:00:00	0.79	125	Yes
		K3		28.12.2020. 08:00:00	28.12.2020. 23:00:00	2.32	178	Yes
		K4		29.12.2020. 08:30:00	29.12.2020. 21:00:00	1.1	199	Yes
		K5		1.1.2021. 13:00:00	2.1.2021. 23:00:00	1.11	179	Yes
		K6		4.1.2021. 11:00:00	4.1.2021. 12:30:00	0.78	208	/

Appendix C

Figure A2 shows all sets of surveys between October 2020 and 14 January 2021 with their respective profile changes.
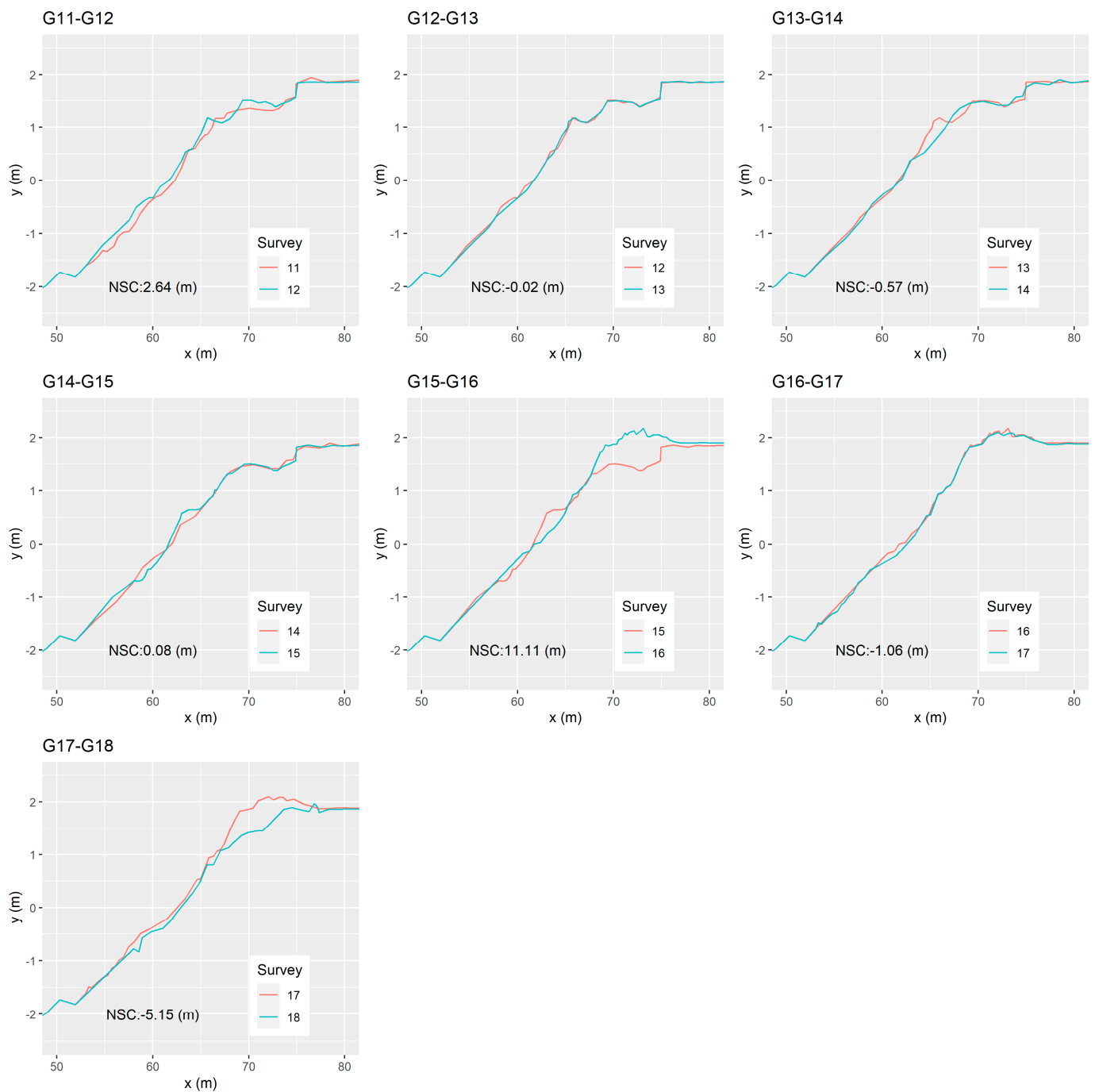
Figure A2. Change in profile sediment distribution for Profile 1 after each geodetic survey 11−18. NSC is short for net sediment change and is calculated by subtracting the earlier from the later survey and summing all values. Only three sets of surveys (G12−G13, G13−G14, and G14−G15) have net sediment change less than 1 m.

Appendix D

By definition from [39], beach orientation is an azimuth (from north) perpendicular to the line connecting the beach endpoints. In the case of the Ploče beach western cell, the beach endpoints are at points A and B located at the root of each groin. Those two points connect the red line in Figure A3, and that line's direction is approximately 129° from north. Perpendicular to that line connecting the endpoints of the beach, and facing offshore, is the beach's orientation in the direction of 219° from north.

Figure A3. Aerial picture of Ploče beach showing a red line connecting end points (A and B) of the western beach cell, a yellow arrow pointing north, and a purple arrow perpendicular to the red line connecting beach endpoints (A and B) and in the direction of the beach orientation, which closes an angle of 219° from north.

References

1. Zadel, Z. Beaches in the Function of Primary Resource of the Beach Tourism Product. *JMTS* **2016**, *51*, 117–130. [CrossRef]
2. Kovačić, M.; Srećko, F.; Perišić, M. The Issue of Coastal Area Management in Croatia: Beach Management. *Acad. Tur.* **2010**, *3*, 53–63.
3. Hanson, H.; Brampton, A.; Capobianco, M.; Dette, H.H.; Hamm, L.; Laustrup, C.; Lechuga, A.; Spanhoff, R. Beach Nourishment Projects, Practices, and Objectives—A European Overview. *Coast. Eng.* **2002**, *47*, 81–111. [CrossRef]
4. Speybroeck, J.; Bonte, D.; Courtens, W.; Gheskiere, T.; Grootaert, P.; Maelfait, J.-P.; Mathys, M.; Provoost, S.; Sabbe, K.; Stienen, E.W.M.; et al. Beach Nourishment: An Ecologically Sound Coastal Defence Alternative? A Review. *Aquat. Conserv. Mar. Freshw. Ecosyst.* **2006**, *16*, 419–435. [CrossRef]
5. Pagán, J.I.; López, M.; López, I.; Tenza-Abril, A.J.; Aragonés, L. Study of the Evolution of Gravel Beaches Nourished with Sand. *Sci. Total Environ.* **2018**, *626*, 87–95. [CrossRef] [PubMed]
6. Pikelj, K.; Ružić, I.; Ilić, S.; James, M.R.; Kordić, B. Implementing an Efficient Beach Erosion Monitoring System for Coastal Management in Croatia. *Ocean Coast. Manag.* **2018**, *156*, 223–238. [CrossRef]
7. Stéphan, P.; Suanez, S.; Fichaut, B.; Autret, R.; Blaise, E.; Houron, J.; Ammann, J.; Grandjean, P. Monitoring the Medium-Term Retreat of a Gravel Spit Barrier and Management Strategies, Sillon de Talbert (North Brittany, France). *Ocean Coast. Manag.* **2018**, *158*, 64–82. [CrossRef]
8. Stocker, T.F.; Qin, D.; Plattner, G.-K.; Tignor, M.M.B.; Allen, S.K.; Boschung, J.; Naules, A.; Xia, Y.; Bex, V.; Midgley, P.M. (Eds.) *Climate Change 2013: The Physical Science Basis. Contribution of Working Group I to the Fifth Assessment Report of the Intergovernmental Panel on Climate Change*; Cambridge University Press: Cambridge, UK; New York, NY, USA, 2014; ISBN 978-1-107-05799-9.
9. Belušić Vozila, A.; Güttler, I.; Ahrens, B.; Obermann-Hellhund, A.; Telišman Prtenjak, M. Wind over the Adriatic Region in CORDEX Climate Change Scenarios. *J. Geophys. Res. Atmos.* **2019**, *124*, 110–130. [CrossRef]
10. Belušić Vozila, A.; Telišman Prtenjak, M.; Güttler, I. A Weather-Type Classification and Its Application to Near-Surface Wind Climate Change Projections over the Adriatic Region. *Atmosphere* **2021**, *12*, 948. [CrossRef]
11. Benetazzo, A.; Fedele, F.; Carniel, S.; Ricchi, A.; Bucchignani, E.; Sclavo, M. Wave Climate of the Adriatic Sea: A Future Scenario Simulation. *Nat. Hazards Earth Syst. Sci.* **2012**, *12*, 2065–2076. [CrossRef]
12. Denamiel, C.; Pranić, P.; Quentin, F.; Mihanović, H.; Vilibić, I. Pseudo-Global Warming Projections of Extreme Wave Storms in Complex Coastal Regions: The Case of the Adriatic Sea. *Clim. Dyn.* **2020**, *55*, 2483–2509. [CrossRef]

13. Bonaldo, D.; Bucchignani, E.; Pomaro, A.; Ricchi, A.; Sclavo, M.; Carniel, S. Wind Waves in the Adriatic Sea under a Severe Climate Change Scenario and Implications for the Coasts. *Int. J. Climatol.* **2020**, *40*, 5389–5406. [CrossRef]
14. Međugorac, I.; Pasarić, M.; Güttler, I. Will the Wind Associated with the Adriatic Storm Surges Change in Future Climate? *Appl. Clim.* **2021**, *143*, 1–18. [CrossRef]
15. Vilibić, I.; Šepić, J.; Pasarić, M.; Orlić, M. The Adriatic Sea: A Long-Standing Laboratory for Sea Level Studies. *Pure Appl. Geophys.* **2017**, *174*, 3765–3811. [CrossRef]
16. Pasarić, M.; Orlić, M. Meteorological Forcing of the Adriatic: Present vs. Projected Climate Conditions. *Geofizika* **2004**, *21*, 69–87.
17. Lončar, G.; Krvavica, N.; Šepić, J.; Bekić, D.; Gašparović, M.; Kulić, T. Potencijal primjene javno dostupnih baza podataka u svrhu procjene opasnosti od poplava mora u priobalnim gradovima Republike Hrvatske. *Hrvat. Vode* **2022**, *30*, 185–200.
18. Vousdoukas, M.I.; Voukouvalas, E.; Annunziato, A.; Giardino, A.; Feyen, L. Projections of Extreme Storm Surge Levels along Europe. *Clim. Dyn.* **2016**, *47*, 3171–3190. [CrossRef]
19. Bujak, D.; Bogovac, T.; Carević, D.; Ilic, S.; Lončar, G. Application of Artificial Neural Networks to Predict Beach Nourishment Volume Requirements. *JMSE* **2021**, *9*, 786. [CrossRef]
20. McCall, R.T.; Masselink, G.; Poate, T.G.; Roelvink, J.A.; Almeida, L.P. Modelling the Morphodynamics of Gravel Beaches during Storms with XBeach-G. *Coast. Eng.* **2015**, *103*, 52–66. [CrossRef]
21. McCall, R.T.; Masselink, G.; Poate, T.G.; Roelvink, J.A.; Almeida, L.P.; Davidson, M.; Russell, P.E. Modelling Storm Hydrodynamics on Gravel Beaches with XBeach-G. *Coast. Eng.* **2014**, *91*, 231–250. [CrossRef]
22. Almeida, L.P.; Masselink, G.; McCall, R.; Russell, P. Storm Overwash of a Gravel Barrier: Field Measurements and XBeach-G Modelling. *Coast. Eng.* **2017**, *120*, 22–35. [CrossRef]
23. Ions, K.; Karunarathna, H.; Reeve, D.E.; Pender, D. Gravel Barrier Beach Morphodynamic Response to Extreme Conditions. *JMSE* **2021**, *9*, 135. [CrossRef]
24. Poate, T.G.; McCall, R.T.; Masselink, G. A New Parameterisation for Runup on Gravel Beaches. *Coast. Eng.* **2016**, *117*, 176–190. [CrossRef]
25. Bergillos, R.J.; Masselink, G.; Ortega-Sánchez, M. Coupling Cross-Shore and Longshore Sediment Transport to Model Storm Response along a Mixed Sand-Gravel Coast under Varying Wave Directions. *Coast. Eng.* **2017**, *129*, 93–104. [CrossRef]
26. Brown, S.I.; Dickson, M.E.; Kench, P.S.; Bergillos, R.J. Modelling Gravel Barrier Response to Storms and Sudden Relative Sea-Level Change Using XBeach-G. *Mar. Geol.* **2019**, *410*, 164–175. [CrossRef]
27. Grottoli, E.; Bertoni, D.; Ciavola, P. Short- and Medium-Term Response to Storms on Three Mediterranean Coarse-Grained Beaches. *Geomorphology* **2017**, *295*, 738–748. [CrossRef]
28. Williams, J.J.; Buscombe, D.; Masselink, G.; Turner, I.L.; Swinkels, C. Barrier Dynamics Experiment (BARDEX): Aims, Design and Procedures. *Coast. Eng.* **2012**, *63*, 3–12. [CrossRef]
29. López de San Román-Blanco, B.; Coates, T.T.; Holmes, P.; Chadwick, A.J.; Bradbury, A.; Baldock, T.E.; Pedrozo-Acuña, A.; Lawrence, J.; Grüne, J. Large Scale Experiments on Gravel and Mixed Beaches: Experimental Procedure, Data Documentation and Initial Results. *Coast. Eng.* **2006**, *53*, 349–362. [CrossRef]
30. Lončar, G.; Carević, D.; Ilić, S.; Krvavica, N.; Kalinić, F. Morfodinamika šljunčanog žala Ploče u uvjetima jakog juga. *Hrvat. Vode* **2020**, *28*, 205–216.
31. Lončar, G.; Kalinić, F.; Carević, D.; Bujak, D. Numerical Modelling of the Morphodynamics of the Ploče Gravel Beach in Rijeka. *e-GFOS* **2021**, *12*, 33–48. [CrossRef]
32. Tadić, A.; Ružić, I.; Krvavica, N.; Ilić, S. Post-Nourishment Changes of an Artificial Gravel Pocket Beach Using UAV Imagery. *JMSE* **2022**, *10*, 358. [CrossRef]
33. Holman, R.A.; Stanley, J. The History and Technical Capabilities of Argus. *Coast. Eng.* **2007**, *54*, 477–491. [CrossRef]
34. Bujak, D.; Ilic, S.; Miličević, H.; Carević, D. Wave Runup Prediction and Alongshore Variability on a Pocket Gravel Beach under Fetch-Limited Wave Conditions. *J. Mar. Sci. Eng.* **2023**, *11*, 614. [CrossRef]
35. Powell, K.A. *Predicting Short Term Profile Response for Shingle Beaches*; Hydraulics Research Wallingford: Wallingford, UK, 1990.
36. Roelvink, D.; Reniers, A.; van Dongeren, A.; van Thiel de Vries, J.; McCall, R.; Lescinski, J. Modelling Storm Impacts on Beaches, Dunes and Barrier Islands. *Coast. Eng.* **2009**, *56*, 1133–1152. [CrossRef]
37. van Rijn, L.C.; Walstra, D.J.R.; Grasmeijer, B.; Sutherland, J.; Pan, S.; Sierra, J.P. The Predictability of Cross-Shore Bed Evolution of Sandy Beaches at the Time Scale of Storms and Seasons Using Process-Based Profile Models. *Coast. Eng.* **2003**, *47*, 295–327. [CrossRef]
38. Hazen, A. Some Physical Properties of Sands and Gravels, with Special Reference to Their Use in Filtration. In *Volume II State Sanitation: A Review of the Work of the Massachusetts State Board of Health, Volume II*; Harvard University Press: Cambridge, MA, USA, 2013; pp. 232–248. ISBN 978-0-674-60048-5.
39. Engstrom, W. A Method of Predicting Beach Orientation. *Prof. Geogr.* **1973**, *25*, 12–15. [CrossRef]